Modulation of Reconstituted Pig Kidney Na^+/K^+-ATPase Activity by Cholesterol in Endogenous Lipid Vesicles: Role of Lipid Domains†

Francisco J. Cuevas,‡ David M. Jameson,§ and Carlos P. Sotomayor*,‡

Instituto de Química, Pontificia Universidad Catolica de Valparaiso, Av. Brasil 2950, Valparaíso, Chile, and Department of Cell and Molecular Biology, John A. Burns School of Medicine, University of Hawaii, Honolulu, Hawaii 96822

Received July 4, 2006; Revised Manuscript Received September 17, 2006

ABSTRACT: Diverse experimental and theoretical evidence suggests that plasma membranes contain cholesterol-induced segregated domains that could play a key role in the modulation of membrane functions, including intrinsic enzyme activity. To gain insight into the role of cholesterol, we reconstituted pig kidney Na^+/K^+-ATPase into unilamellar vesicles of endogenous lipids mimicking the natural membrane and addressed the question of how modification of the cholesterol content could affect the ATPase activity via changes in the membrane lipid phase and in the protein structure and dynamics. We used steady-state and time-resolved fluorescence spectroscopy with the lipid phase probes DPH and Laurdan and the protein probe fluorescein and also used infrared spectroscopy using attenuated total reflectance. Upon modification of membrane cholesterol content, the ATPase activity did not change monotonically but instead exhibited abrupt changes resulting in two peaks at or close to critical cholesterol mole fractions (25 and 33.3 mol %) predicted by the superlattice or regular distribution model. Fluorescence parameters associated with the membrane probes also showed abrupt changes with peaks, coincident with the cholesterol concentrations associated with the peaks in the enzyme activity, while parameters associated with the protein probes also showed slight but abrupt changes resulting in dips at the same cholesterol concentrations. Notably, the IR amide I band maximum also showed spectral shifts, characterized by a frequency variation pattern with peaks at the same cholesterol concentrations. Overall, these results indicate that the lipid phase had slightly lower hydration, at or near the two critical cholesterol concentrations predicted by the superlattice theory. However, in the protein domains monitored there was a slight but significant hydration increase along with increased peptide backbone flexibility at these cholesterol concentrations. We propose that in the vicinity of the critical mole fractions, where superlattice formation can occur, minute changes in cholesterol concentration produce abrupt changes in the membrane organization, increasing interdomain surfaces. These changes, in turn, induce small changes in the protein's structure and dynamics, therefore acting to fine-tune the enzyme.

Na^+/K^+-ATPase[1] carries Na^+ and K^+ ions across the plasma membrane of cells against their respective electrochemical gradients, at the expense of the free energy of ATP hydrolysis (*1*, *2*). During this transport process, ATPase undergoes cyclic conformational changes between different reactive states (*3*). The idea that the physical state or the properties of the membrane lamella influence the enzyme's activity, as well as the functioning of other intrinsic membrane proteins, has been accepted as a plausible hypothesis. Evidence for this hypothesis has been gathered over the last few decades (*4*−*8*); however, at the molecular level the underlying processes are not well understood. The activity of membrane-bound enzymes was at first related to the fluidity and other bulk properties of the lipid bilayer (*5*, *7*, *8*). Different types of evidence, however, suggested that plasma membranes contain segregated domains that could play a key role in the modulation of membrane functions, including intrinsic enzyme activity (*9*−*13*). In this regard, there is increasing agreement with the hypothesis that cholesterol has a crucial role in the segregation of membrane domains (*14*).

However, a new aspect emerged from investigations of problems related to the influence of cholesterol in the segregation of the lipid components into immiscible fluid domains. In a theoretical development, Mouritsen, Zuckermann, and co-workers (*15*−*17*) postulated that, in addition to the two well-established phases of a lipid-bilayer system, the low-temperature *gel* phase, so, and the fluid high-temperature *liquid-crystalline* phase, ld, cholesterol promotes the formation of a third phase that coexists with the former. This new intermediate fluid phase, referred to as "*liquid-*

† This work was supported by MECESUP and CONICYT (to F.J.C.) and DI-PUCV.

* Author to whom correspondence should be addressed. Tel: 56-32-2273171. Fax: 56-32-2273422/2273420. E-mail: psotomay@ucv.cl.

‡ Pontificia Universidad Catolica de Valparaiso.

§ University of Hawaii.

[1] Abbreviations: Na^+/K^+-ATPase, sodium- and potassium-activated adenosinetriphosphatase; ATP, adenosine 5′-triphosphate; FITC, fluorescein isothiocyanate; IAF, 5-iodoacetamidofluorescein; DPH, 1,6-diphenyl-1,3,5-hexatriene; Laurdan, 2-(dimethylamino)-6-lauroylnaphthalene; BSA, bovine serum albumin; $C_{12}E_8$, octaethylene glycol dodecyl ether; PC, phosphatidylcholine; PE, phosphatidylethanolamine; PI, phosphatidylinositol; CHO, cholesterol; GP, generalized polarization; DHE, dehydroergosterol; TCA, trichloroacetic acid; FTIR-ATR, infrared spectroscopy with the attenuated total reflectance technique.

10.1021/bi061351e CCC: $33.50 © 2006 American Chemical Society
Published on Web 10/26/2006

ordered" phase, lo, exhibits translational degrees of freedom of the lipid molecules that are similar to those in a conventional fluid bilayer state, while the conformational degrees of freedom of the lipid hydrocarbon chains resemble those of the gel state. The experimental data and the theoretical considerations were used to obtain phase diagrams of cholesterol-containing lamellas (*18*). These developments provided the theoretical foundation and empirical evidence for the hypothesis that fluid segregated domains could coexist in model and biological membranes, in physiological conditions, when cholesterol is present in the proper amount.

Another line of investigation regarding the segregation of fluid domains arose from experimental evidence obtained from fluorescence studies performed in phospholipid bilayers with bulky guest molecules such as pyrene-PC and sterols (*19*−*22*). Specifically, three different fluorescence parameters, the excimer to monomer fluorescence ratio of pyrene-PC, the fluorescence intensity of DHE (dehydroergosterol), and the general polarization of Laurdan [2-(dimethylamino)-6-lauroylnaphthalene], showed peculiar nonmonotonic behaviors. Concentration-induced abrupt changes were observed, resulting in local maxima or minima at certain critical concentrations of pyrene-PC (*20*, *21*), DHE (*22*), and cholesterol (*19*), respectively. These results were interpreted in terms of the superlattice or regular distribution model proposed by Sommerharju and co-workers (*21*, *23*) and extended by Chong and co-workers (*21*, *22*), which considers the coexistence of segregated domains exhibiting different lattice arrangements of sterol (or bulky molecule) and lipid molecules. Specifically, according to the sterol regular distribution model (*22*), the cholesterol molecules tend to be regularly distributed in a hexagonal host lipid lattice, forming a superlattice, to maximize separation from each other. Due to thermal fluctuations, changes in bilayer curvature, and the presence of impurities, irregular distributions always coexist with regular distributions, forming segregated domains, but the ratios of regular to irregular regions reach local maxima at critical cholesterol mole fractions. Membrane-free volume is less abundant in regular regions than in irregular regions, due to tighter molecular packing in the former. As there are many critical mole fractions over a wide range of sterol concentrations, membrane-free volume varies with sterol mole fraction in a periodic manner, with local minima at critical sterol mole fractions. Thus, it is has been hypothesized that membrane properties, especially those influenced by membrane-free volume (or membrane defects), are modulated by sterol content in an alternating manner by minute changes in lipid composition on either side of a critical mole fraction (ref *24* and references cited therein). Sterol regular distribution (superlattice) formation was first considered to result from long-range pairwise repulsive forces between bulky steroids rings, maximizing separation from each other (*22*, *23*). Recent developments indicated, however, that, in addition to these repulsive forces, short-range multibody attractive interactions between sterol and phospholipids are necessary for supperlattice formation (*25*, *26*).

The existence of segregated domains with fluid characteristics in lipid lamellas and the role of cholesterol in their formation have been intriguing aspects in this field. As already discussed, different theoretical developments and corresponding empirical evidence indicated the feasibility of such domains. However, compelling proof remained elusive until Dietrich et al. (*27*) obtained direct microscopic visualization of segregated fluid domains of micrometer dimensions. This visualization was achieved in supported bilayers and in unsupported giant unilamellar vesicles (GUV) containing phospholipids, sphingolipids, and cholesterol. Interestingly, in one of the two models utilized, these domains were visualized when the temperature was lowered through 25 °C. At the physiological temperature of 37 °C no discrete domains were microscopically visible. However, fluorescence quenching studies performed in systems of similar composition indicated the coexistence of segregated domains at 37 °C (*28*). Considering the time scale of the excited-state lifetime of the fluorophores, on the order of nanoseconds, fluorescence quenching experiments monitor events at smaller distance scales (nanometer) than fluorescence microscopy. These and other results obtained by single molecule optical techniques and pulse EPR spin-labeling methods (*29*) suggest that cholesterol may induce, in some conditions, the segregation of fluid domains of very small dimensions and/or with quite short lifetimes. On the other hand, in the past decade, evidence has been found for regular distributions in different lipid membranes (reviewed in ref *30*). Specifically, in relation to membrane-related enzymes, studies of two membrane surface acting enzymes, phospholipase A2 and cholesterol oxidase, in model membranes have shown a nonmonotonical composition-driven regulation; i.e., the activities of both enzymes are modulated in an alternating manner by membrane cholesterol content modification (*24*, *31*). Also, Cannon et al. reported that headgroup superlattices may regulate the activity of the sarcoplasmic reticulum channel protein from cardiac myocytes reconstituted in planar lipid bilayers composed of POPC and POPE (*32*).

Na^+/K^+-ATPase activity is known to be affected by membrane cholesterol content (*4*, *33*−*36*). Early experiments showed inhibition of activity by high levels of membrane cholesterol (*35*, *36*). In a later study of cholesterol's effect on Na^+/K^+-ATPase activity in bovine kidney basolateral membranes, Yeagle et al. (*4*) reported that maximal activity is observed at the native membrane cholesterol content. When the cholesterol content of the membranes was above or below that found in the native membrane, the enzyme activity decreased. Cornelius, in a study on reconstituted shark Na^+/K^+-ATPase (*33*), reported a stimulatory effect at low cholesterol concentration and an inhibitory effect at high concentration. We found that Na^+/K^+-ATPase in pig kidney basolateral membrane preparation showed a nonmonotonic activity dependence with cholesterol content, producing a biphasic change in activity with a maximum at the native membrane cholesterol content (*37*). To gain insight into the mechanism of cholesterol's effect, we used several hydrophobic fluorescent probes, which insert into different regions of the membrane bilayer, and reported on the degree of hydration of their environment. The results, in agreement with the regular distribution model, indicated nonmonotonic variations of the fluorescence parameters with increasing cholesterol concentration, suggesting that membranes with the native cholesterol content have a minimum hydration in the bulk lipid phase and maximum hydration at the protein−lipid interface.

In the present investigation, we addressed the problem of how changes in the membrane lipid phase and in the enzyme

properties, due to modification of the cholesterol content, may affect the ATPase activity of reconstituted Na^+/K^+-ATPase in model membranes. Highly purified pig kidney enzyme was reconstituted into unilamellar vesicles of a mixture of phosphatidylcholine, phosphatidylethanolamine, and phosphatidylinositol of bovine natural lipids, mimicking the proportion of the natural membrane where cholesterol content was modified. We employed the lipid phase probes DPH and Laurdan and the protein probe fluorescein bound to a lysine residue at or near the active site (using FITC) and to cysteines localized in cytoplasmatic domains that presumably experience significant environment changes (using IAF). Infrared spectroscopy using the attenuated total reflectance technique, FTIR-ATR, was also used to study protein conformational changes and lipid phase organization.

MATERIALS AND METHODS

Materials. ATP, EDTA, histidine, sucrose, BSA, octaethylene glycol dodecyl ether ($C_{12}E_8$), and sodium dodecyl sulfate were obtained from Sigma (St. Louis, MO). 1,6-Diphenyl-1,3,5-hexatriene (DPH), 1-(4-trimethylammoniumphenyl)-6-phenyl-1,3,5-hexatriene, 2-(dimethylamino)-6-lauroylnaphthalene (Laurdan), fluorescein isothiocyanate isomer I (FITC), and 5-iodoacetamidofluorescein (IAF) were obtained from Molecular Probes (Eugene, OR), Bio-Beads SM-2 were obtained from Bio-Rad (Irvine, CA). All lipids and cholesterol were obtained from Avanti Polar Lipids (Alabaster, AL). All other chemicals used were of analytical or spectroscopic grade and were obtained from commercial sources.

Membrane Preparation. Na^+/K^+-ATPase-rich membranes were prepared from the outer medulla of pig kidney according to the procedure of Jørgensen (*38*, *39*) as previously described (*37*). This method yields partially purified enzyme in the form of membrane fragments rich in Na^+/K^+-ATPase, containing about 0.6 mg of phospholipid and 0.2 mg of cholesterol/mg of protein. The specific ATPase activity was determined in a medium containing 30 mM Tris, pH 7.4, 3 mM ATP, 1 mM EGTA, 8.2 mg/mL NaCl, 1.1 mg/mL KCl, and 0.67 mg/mL $MgCl_2$. The reaction was stopped by addition of TCA. Inorganic phosphate generated by this reaction was quantified according to Baginsky procedures (*40*). The protein concentrations in membranes and vesicles were determined by the method of Lowry et al. (*41*), including the quantitative precipitation of the protein with TCA, and SDS was used for lipid solubilization. Bovine serum albumin was used as a standard. Suspensions of Na^+/K^+-ATPase-rich membrane fragments (about 5 mg/mL of protein) in buffer (30 mM histidine, pH 7.4, 1 mM EDTA, and 3 mM ATP) were quickly frozen in liquid nitrogen in samples of 500 μL and stored at −80 °C.

Solubilization and Reconstitution. Solubilization and reconstitution of Na^+/K^+-ATPase were achieved using the method described by Cornelius for shark Na^+/K^+-ATPase, yielding unilamellar vesicles with average diameters around 2200 Å (*42*). Initially, membrane-bound Na^+/K^+-ATPase was solubilized using the nonionic detergent $C_{12}E_8$. Next, the lipids of choice were solubilized using the same detergent, and the two solutions were mixed in a proportion to obtain a protein:lipid weight ratio of 1:20, allowing ample time before the next step in order to create a uniform lipid protein distribution. Vesicles containing reconstituted Na^+/K^+-ATPase spontaneously formed when the detergent was subsequently removed by addition of hydrophobic Bio-Beads and incubated at 4 °C during 12 h. Enzyme activity was measured during enzyme solubilization and reconstitution to check that solubilization and reconstitution were achieved without loss of activity. After reconstitution, the cholesterol and phospholipid content of the vesicles remained virtually unchanged from the initial ratio as determined by a cholesterol oxidase assay (*43*) and the method of Zilversmith and Davis (*44*), respectively. Enzyme activity was measured after reconstitution to determine the fraction of each of the possible orientations, i.e., right-side-out oriented enzyme (r/o) that has the ATP site shielded inside the vesicles, inside-out oriented enzyme (i/o) that has the ATP site exposed to the medium, and nonoriented enzyme (n/o) with both sides exposed. The latter can be due to very leaky vesicles or externally adsorbed enzyme (*45*). This determination was accomplished according to the protocol of Cornelius (*46*), measuring first the total activity in reopened vesicles by detergent addition, second the activity in sealed vesicles, and third the activity in sealed vesicles with added ouabain. The K^+ ionophore valiomycin, in combination with an H^+ ionophore, was also used in the last two experiments in order to permit the K^+ to leak back in once it has been pumped out.

FITC and IAF Labeling. Both labeling procedures were performed in purified membrane fragments. The Na^+/K^+-ATPase was modified by FITC using the proceedure of Ward and Cavieres (*47*). Namely, a sample of purified membrane-bound enzyme was incubated at 20 °C, in the dark, at 1.0 mg/mL protein in a buffer of Tris, pH 9.2, and 150 mM NaCl and for a period up to 3 h with 50 μM FITC. The protein was modified by IAF using the procedure of Kapakos and Steinberg (*48*). Namely, the protein was incubated at 20 °C, in the dark, at 1.5 mg/mL protein in a buffer of 30 mM histidine, pH 7.4, and 20 mM KCl with 100 μM IAF for a period of 4 h. In order to separate free probe, both samples were spun down, washed, and resuspended in fresh buffer by ultracentrifugation at 35000 rpm. Control labeling experiments in the presence of ATP for the FITC labeling and in the absence of K^+ for IAF labeling were performed. The activity of both labeled enzymes was also determined.

Time-Resolved Fluorescence Measurements. Measurements were performed at the Laboratory for Fluorescence Dynamics at the University of Illinois at Urbana−Champaign, IL, using a multifrequency phase and modulation fluorometer. For DPH the exciting light was from a Coherent Nd:YAG mode-locked laser pumping a rhodamine dye laser. The dye laser was tuned to 690 nm, which was then frequency doubled to 345 nm. Emission was observed through a Schott KV-399 long band-pass filter and a Corning TB-400 band-pass filter to isolate emission from DPH and block scattered light. For fluorescein probes, the exciting light was from an argon ion laser at 488 nm, and the emission was observed through a Schott OG-530 long band-pass filter. In all lifetime measurements, the exciting light was polarized parallel to the vertical laboratory axis, and the emission was viewed through a Glan-Thompson polarizer oriented at 55° (*49*). Phase and modulation values were obtained as previously described (*50*−*52*), at 12 modulation frequencies in the interval 3−110 MHz and 20−150 MHz for DPH and

fluorescein, respectively. Dimethyl-POPOP in ethanol (τ = 1.45 ns) and fluorescein in 0.001 N NaOH (τ = 4.05 ns) were used as a reference lifetime standards. For fluorescein probes, dynamic polarization measurements were also carried out.

Data Analysis. Time-resolved fluorescence data were analyzed using the Globals Unlimited software package (Laboratory for Fluorescence Dynamics, University of Illinois at Urbana−Champaign, Urbana, IL). The DPH phase and modulation data were analyzed either by assuming a sum of discrete exponentials (*51*) or by continuous distribution models which assumed Lorentzian or Gaussian distributions (*50*−*54*). For fluorescein probes, phase and modulation data were also analyzed using the asymmetric distribution model (*53*). According to Klonis and Sawyer, this is a useful empirical model for analyzing the emission decay of fluorescein labeled molecules (*55*).

$$p(\tau) = \frac{1}{\tau}\left\{\ln\left[\frac{\tau(\tau_u - \tau_L)}{\tau_u(\tau - \tau_L)}\right]\right\}^{\beta} \quad (1)$$

In this analysis, the τ_L and τ_u parameters, which represent the lower and upper lifetime limits of the asymmetric distribution, reflect the quenched and unquenched lifetimes, respectively. β is the density-of-state parameter that describes the distribution of lifetimes between the two limits.

Fluorescein anisotropy decay data, i.e., dynamic polarization data, which include phase angles and modulation ratios, obtained with perpendicular and parallel oriented sinusoidal polarized light, were fit to the following models of anisotropy decay:

hindered rotator model

$$r(t) = (r_0 - r_\infty)\exp(-t/\phi_F) + r_\infty \quad (2)$$

where r_0 is the amplitude of the anisotropy decay at time 0, ϕ is the rotational correlation time of the anisotropy decay, and r_∞ is the residual anisotropy at infinite time.

nonassociative two-component anisotropy decay model

$$r(t) = r_0 f_{xb}\exp(-t/\phi_F) + r_0(1 - f_{xb})\exp(-t/\phi_S) \quad (3)$$

where ϕ_F and ϕ_S are the rotational correlation times associated with the fast and slow decay processes of the anisotropy decay, respectively, and f_{xb} is the fraction of the anisotropy decay associated with the fast decay processes (*56*). The goodness of fit of the data to a particular model was judged by the value of the reduced chi square (χ^2). Analyses were performed using a constant, frequency-independent standard deviation of 0.2° for phase angles and 0.004 for modulation ratios. Correlated error analyses (i.e., one parameter is varied near the χ^2 minimum while the other parameters are all free) were performed on the lifetimes, and the rigorous 67% confidence limits are reported for each parameter.

Laurdan Fluorescence. The generalized polarization of Laurdan, utilized to assess its fluorescence spectral shifts, was measured as previously described (*10*, *57*). Briefly, the generalized polarization (GP) is defined as

$$GP = (I_{440} - I_{490})/(I_{440} + I_{490}) \quad (4)$$

where I_{440} and I_{490} are the fluorescence intensities at 440 nm (gel phase emission maximum) and 490 nm (liquid crystalline phase emission maximum), respectively, upon excitation at 360 nm.

ATR-FTIR Sample Preparation. Supported planar bilayers adsorbed onto an ATR germanium plate were obtained from vesicles with reconstituted protein, which were incubated for 90 min over the germanium plate, in the presence of 150 mM NaCl and 50 mM $CaCl_2$ according to Silvestro and Axelsen (*58*). The adsorbed fragments were washed three times with 30 mM phosphate buffer, pH 7.4, in D_2O. Spectra were recorded 2 h after sample preparation.

ATR-FTIR Measurements. Spectra were scanned in single beam mode using a Spectrum One FTIR spectrometer from Perkin-Elmer equipped with a DTGS detector and continuously purged with dry air. The samples were adsorbed bilayers on a germanium ATR plate with an angle of incidence of 45°. Typically 256 interferograms with 1 cm^{-1} resolution and a scan rate of 0.1 cm^{-1}/s were collected and averaged. To eliminate the contribution of the aqueous phase, background spectra were measured before adsorption of the lipid bilayers, with the cell above the germanium plate filled with 30 mM phosphate buffer, pH 7.4, in D_2O; background scans were stored in the computer memory for further use. Sample spectra were recorded with the same buffer at 37 °C. The smoothing and deconvolution of spectra were performed with GRAMS RESEARCH version 3.01C of Galactic Industries Corp.

RESULTS

Characterization of Reconstituted Na^+/K^+-ATPase. SDS−PAGE analysis of the Na^+/K^+-ATPase during purification indicated that the enzyme was purified to a level of 95−97% in the solubilized state. The ratio of the two characteristic bands of this protein, 96 and 56 kDa, was 3.0 in accordance with Jorgensen (*59*), who reported values of 2.8 and 3.0 for the α/β mass ratio determined by the Lowry method and by quantitative amino acid analysis, respectively. The enzyme was reconstituted into unilamellar vesicles where the cholesterol content was modified to between 22 and 35 mol %; the phospholipids were composed of a constant mixture of PC:PE:PI = 78:19:3, which is about the ratio found in the corresponding natural membrane. For comparison purposes, enzyme was also reconstituted into vesicles of pure PC with the same cholesterol content. For all reconstitutions an initial protein to lipid ratio of 1:20 was utilized and a protein recovery after reconstitution of 75−80% was obtained, which was independent of cholesterol content. The sidedness or orientation of the reconstituted enzyme in the vesicle membrane was determined, according to Cornelius (*42*) (see Materials and Methods), to be 72−75% of right side out, 8−10% of inside out, and 15−19% of nonoriented; the handedness was the same for both types of vesicles. The orientation of the reconstituted enzyme was independent of the cholesterol content, in accordance with Cornelius (*33*).

The ATPase activity of the enzyme was determined in all purification steps and reconstitution and was 14−16 UI/mg in the purified natural membranes, 10 UI/mg upon solubilization, and 15 UI/mg upon reconstitution in PC vesicles without cholesterol, indicating that the reconstitution was

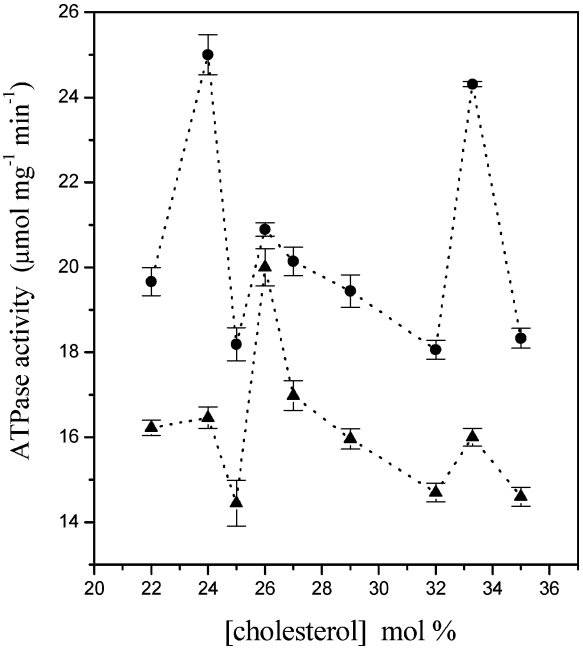

FIGURE 1: ATPase activity of pig kidney basolateral membrane Na^+/K^+-ATPase reconstituted in unilamellar vesicles of natural lipids, as a function of membrane cholesterol content, at 37 °C. Key: (●) PC:PE:PI:CHO vesicles; (▲) PC:CHO vesicles. Each point represents an average of data in duplicate and standard error.

achieved without loss of activity. This activity was probed after opening the closed vesicles by addition of the detergent $C_{12}E_8$ in the presence of Na^+, K^+, Mg^{2+}, and ATP. The dependence of the ATPase activity at 37 °C on membrane cholesterol content is shown in Figure 1. A general trend of a slight increase up to 26 mol % followed by slight decrease is apparent in both curves in the cholesterol range from 22 to 35 mol %. This trend has been reported previously by Cornelius for reconstituted shark Na^+/K^+-ATPase using large cholesterol concentration increments (*33*). In contrast to previous studies, in this work small cholesterol concentration increments (1 mol %) were used, and the ATPase activity did not change monotonically with cholesterol content modification; instead, the activity exhibited abrupt changes resulting in two peaks at 24 and 33.3 cholesterol mol % for vesicles with the lipid mixture PC:PE:PI and at 26 and 33.3 mol % for PC vesicles. These peak positions are at or close to the critical cholesterol mole fractions (i.e., 25 and 33.3 mol %) predicted by the superlattice or regular distribution model (*20*−*23*).

Steady-State Fluorescence Measurements. The effect of modification of the vesicle cholesterol content on the membrane properties was studied, at 37 °C, in the absence and presence of reconstituted Na^+/K^+-ATPase. The shifts of Laurdan's emission spectra, as a function of membrane cholesterol content, were followed using the generalized polarization parameter (GP) as given in Table 1. In both types of vesicles without protein a general trend characterized by a slight increase of GP is observed, while in vesicles with reconstituted protein a slight decrease is apparent. In PC:CHO vesicles this decrease is very slight and occurred up to 32 mol %. Protein reconstitution induced a general increase of Laurdan GP in PC:PE:PI vesicles, while a considerable decrease was observed in PC vesicles. Interestingly, Laurdan GP did not change monotonically with the

Table 1: General Polarization of Laurdan Fluorescence Embedded in Natural Lipid Unilamelar Vesicles with and without Reconstituted Pig Kidney Na^+/K^+-ATPase as a Function of Membrane Cholesterol Content at 37 °C[a]

	GP	
[CHO] (mol %)	PC:CHO	PC:CHO:ATPase
22	0.080 ± 0.002	−0.085 ± 0.002
24	0.085 ± 0.003	−0.081 ± 0.003
25	0.083 ± 0.002	−0.083 ± 0.002
26	0.100 ± 0.003	−0.076 ± 0.003
27	0.095 ± 0.003	−0.090 ± 0.003
29	0.088 ± 0.003	−0.088 ± 0.003
32	0.091 ± 0.002	−0.091 ± 0.003
33.3	0.117 ± 0.002	−0.057 ± 0.003
35	0.109 ± 0.004	−0.042 ± 0.004
	GP	
[CHO] (mol %)	PC:PE:PI:CHO	PC:PE:PI:CHO:ATPase
22	0.066 ± 0.001	0.169 ± 0.004
24	0.143 ± 0.001	0.176 ± 0.005
25	0.126 ± 0.001	0.157 ± 0.004
26	0.117 ± 0.001	0.156 ± 0.005
27	0.141 ± 0.003	0.150 ± 0.003
29	0.074 ± 0.001	0.140 ± 0.005
32	0.125 ± 0.004	0.145 ± 0.003
33.3	0.171 ± 0.002	0.163 ± 0.004
35	0.145 ± 0.003	0.155 ± 0.003

[a] Excitation wavelength: 360 nm. Emission wavelengths: 440 and 490 nm. Each point represents an average of data in duplicate and standard error.

increase in cholesterol content. In both systems in the presence of the protein, abrupt changes were observed at the cholesterol concentrations where enzymatic activity peaks were observed; these peaks were clearly conspicuous in the PC:PE:PI:CHO:ATPase system and were coincident with the cholesterol concentrations of 24 and 33.3 mol %, where the enzymatic activity peaks were observed.

Time-Resolved Fluorescence Measurements. Time-resolved fluorescence intensity decay data of DPH embedded in vesicle bilayers were analyzed using different decay models. In all cases, a two-component model consisting of one discrete exponential and one Lorentzian lifetime distribution gave the best fit. A fixed discrete component of 0.001 ns was used to account for scattered light, which was <2% in terms of fractional intensity contribution. The results recovered from the analyses are given in Table 2. DPH fluorescence lifetimes obtained from the Lorentzian distribution centers showed, in all systems, a general increasing trend with increasing membrane cholesterol content; however, these changes were nonmonotonic; in systems without the enzyme, abrupt changes were apparent at 24, 29, and 33.3 mol % for PC:PE:PI:CHO vesicles and at 26 and 33.3 mol % for PC:CHO vesicles. In vesicles with reconstituted enzyme, peaks were less clear or reduced to slope changes. In PC:CHO vesicles a peak was also observed at 24 cholesterol mol %. Measurements done with the DPH derivatives DPH-propionic acid and TMAP-DPH gave the same results related to the general trend of the curve and the abrupt changes with peaks at 24 and 33.3 mol % and at 26 and 33.3 mol % for PC vesicles (data not shown).

Time-resolved fluorescence intensity decay and anisotropy decay measurements of fluorescein conjugated to Na^+/K^+-ATPase lysine and cysteines were also performed. The enzyme was labeled with FITC and with IAF prior to the

Table 2: Fluorescence Decay Parameters of DPH in Natural Lipid Unilamelar Vesicles with and without Reconstituted Pig Kidney Na^+/K^+-ATPase, Effect of Modification of the Membrane Cholesterol Content, and Two-Component Analysis with One Lorentzian Distribution and One Discrete Component[a]

	PC:CHO				PC:CHO:ATPase			
[CHO] (mol %)	center (ns)	width (ns)	f_i	χ^2	center (ns)	width (ns)	f_i	χ^2
22	7.19 (−0.03; +0.05)	1.94 ± 0.17	0.99	1.32	8.22 ± 0.04	2.22 ± 0.21	0.99	0.92
24	7.42 (−0.04; +0.05)	1.55 ± 0.20	0.99	1.16	8.38 ± 0.05	2.86 ± 0.25	0.99	1.26
25	7.45 ± 0.03	2.53 ± 0.13	0.99	0.70	8.15 (−0.03; +0.05)	2.69 ± 0.13	0.99	1.09
26	8.34 (−0.04; +0.05)	2.51 ± 0.16	0.99	1.31	8.76 (−0.04; +0.05)	2.74 ± 0.19	0.99	0.93
27	8.20 (−0.05; +0.07)	2.84 ± 0.11	0.99	1.08	8.80 (−0.04; +0.06)	3.04 ± 0.08	0.99	1.28
29	8.12 ± 0.04	2.55 ± 0.20	0.99	1.19	8.85 (−0.04; +0.06)	3.15 ± 0.22	0.99	0.79
32	8.57 (−0.04; +0.06)	2.49 ± 0.17	0.99	1.16	8.44 (−0.03; +0.06)	2.49 ± 0.17	0.99	1.16
33.3	8.93 (−0.04; +0.05)	2.54 ± 0.07	0.99	1.09	9.01 (−0.03; +0.05)	2.81 ± 0.16	0.99	1.33
35	8.63 (−0.02; +0.05)	2.78 ± 0.14	0.99	0.97	9.00 (−0.03; +0.06)	2.98 ± 0.18	0.99	1.31
	PC:PE:PI:CHO				PC:PE:PI:CHO:ATPase			
[CHO] (mol %)	center (ns)	width (ns)	f_i	χ^2	center (ns)	width (ns)	f_i	χ^2
22	7.93 (−0.03; +0.04)	2.81 ± 0.20	0.99	1.06	7.49 (−0.03; +0.04)	3.21 ± 0.19	0.99	1.11
24	8.35 (−0.04; +0.03)	2.65 ± 0.22	0.99	0.96	7.74 (−0.03; +0.04)	3.05 ± 0.25	0.99	1.10
25	8.25 (−0.03; +0.04)	2.73 ± 0.18	0.99	0.70	7.70 (−0.05; +0.07)	3.15 ± 0.23	0.99	1.05
26	7.30 (−0.03; +0.05)	2.91 ± 0.16	0.99	1.31	7.97 (−0.05; +0.04)	3.19 ± 0.19	0.99	0.98
27	8.12 (−0.05; +0.04)	2.87 ± 0.21	0.99	1.58	7.98 ± 0.05	3.28 ± 0.25	0.99	0.79
29	8.32 (−0.05; +0.04)	2.88 ± 0.23	0.99	1.19	8.01 (−0.03; +0.05)	3.31 ± 0.20	0.99	1.28
32	7.97 ± 0.05	2.89 ± 0.17	0.99	1.26	8.45 (−0.05; +0.04)	3.37 ± 0.18	0.99	1.09
33.3	8.75 (−0.02; +0.04)	2.84 ± 0.17	0.99	1.09	8.48 ± 0.04	3.33 ± 0.16	0.99	1.25
35	8.32 ± 0.05	2.78 ± 0.14	0.98	0.97	8.13 (−0.05; +0.04)	3.25 ± 0.18	0.99	0.83

[a] Center refers to the center of the Lorentzian distribution; width refers to the full width at half-maximum of the distribution, and f_i corresponds to the fractional contribution to the intensity of the distributed component. The minor discrete component was fixed at 0.001 ns to account for scattered light. The reduced chi-square (χ^2) value corresponds to the fit of the phase and modulation data to the model. The errors given in parentheses represent the correlated 67% confidence limits of the reduced χ^2.

solubilization and reconstitution steps, i.e., in the purified membrane-bound state. The stoichiometry of labeling was determined spectroscopically according to Tyson et al. (*60*) to be 1:1 and 3:1 probe:protein for FITC and IAF labeling, respectively. Analysis of the ATPase activity of FITC-labeled enzyme revealed total inactivation upon labeling [consistent with previous observations (*47*)]. A control experiment indicated, moreover, that the enzyme was not labeled with FITC in the presence of ATP. On the other hand, IAF labeling induced only a 15% ATPase activity decrease and occurred only in the presence of potassium ions, irrespective to the presence or absence of ATP. The labeled samples were then solubilized, and the enzyme was reconstituted following the same protocol used for unlabeled protein.

In addition to the aforementioned models used with DPH data, fluorescein phase and modulation data were also analyzed with the asymmetric distribution (*54*), which gave the best fit to these data. The results of the analysis are given in Table 3. The fixed discrete component, of 0.001 ns, was also used to account for scattered light. In this asymmetric distribution, the τ_L and τ_u parameters represent the lower and upper lifetime limits of the distribution, and β, the density-of-state parameter, describes the distribution of lifetimes between the two limits. During the analysis all parameters were permitted to float; though, in all cases the recovered values for τ_L were between 0.18 and 0.22 ns. In all cases, the upper lifetime limit, τ_u, accounted for the majority of the emission as judged by negative β values. Fluorescein lifetimes obtained from τ_u showed higher values when bound to cysteines than when bound to the lysine residue, at all cholesterol concentrations. Fluorescein lifetimes also showed, in both systems, nonmonotonic behavior with abrupt dips at 24, 27, and 33.3 cholesterol mol % for PC:PE:PI:CHO vesicles and at 26 and 33.3 mol % for PC:CHO vesicles. These cholesterol concentrations correspond to values where Laurdan PG and/or DPH lifetimes showed peaks.

Dynamic polarization data of FITC- and IAF-labeled enzyme were analyzed by a hindered rotator model and a nonassociative biexponential anisotropy decay model (eqs 1 and 2). The best fit parameters were obtained with the biexponential model, which are given in Table 4; specifically the parameters include r_0, the time zero amplitude, f_{xb} and ϕ_F, the fractional amplitude and rotational correlation time of the fast component, respectively, and ϕ_S, the slow rotational correlation time. The values of the slow rotational correlation time ϕ_S, associated with the rotational diffusion of the whole protein, ranged between 85 and 115 ns for the FITC-labeled enzyme and 68 and 126 ns for the IAF-labeled enzyme. This range of values is smaller than what might be expected from a protein such as Na^+/K^+-ATPase embedded in a membrane. This disparity may reflect the existence of internal motions of intermediate decay rate or arise from the inherent limitation of quantifying rotational correlation times that are on a much slower time scale than the emission lifetime of the reporter group. The recovered time zero anisotropy values and amplitude of the fast decay were similar for both labeled residues and both types of vesicles without significant variations. Although the values of the fast rotational correlation time, ϕ_F, were similar for both labeling sites, this parameter showed nonmonotonic behavior with slight but abrupt significant changes with membrane cholesterol content modification, showing dips at 24 and 33.3 cholesterol mol % for PC:PE:PI vesicles and at 26 and 33.3 mol % for PC vesicles, for both types of labeling. Although the values of the recovered parameters obtained with the

Table 3: Fluorescence Decay Parameters of Fluorescein-Labeled Pig Kidney Na^+/K^+-ATPase Reconstituted in Natural Lipid Unilamelar Vesicles, Effect of Modification of Membrane Cholesterol Content, and Phase and Modulation Data Analyzed according to the Asymmetric Distribution Model[a]

	PC:CHO:ATPase-FITC				PC:CHO:ATPase-IAF			
[CHO] (mol %)	τ_u (ns)	β	f_i	χ^2	τ_u (ns)	β	f_i	χ^2
22	4.34 ± 0.02	−0.57 ± 0.03	0.97	0.20	4.67 ± 0.01	−0.65 ± 0.07	0.99	0.18
24	4.36 ± 0.01	−0.56 ± 0.05	1.00	0.08	4.72 ± 0.01	−0.70 ± 0.02	0.99	0.35
25	4.33 ± 0.01	−0.62 ± 0.01	1.00	0.19	4.82 ± 0.01	−0.67 ± 0.03	0.99	0.38
26	4.31 ± 0.01	−0.64 ± 0.02	1.00	0.25	4.63 ± 0.01	−0.71 ± 0.01	0.99	0.25
27	4.39 ± 0.01	−0.56 ± 0.03	0.99	0.10	4.85 ± 0.01	−0.63 ± 0.01	1.00	0.42
29	4.44 ± 0.01	−0.58 ± 0.02	0.99	0.09	4.74 ± 0.01	−0.64 ± 0.02	1.00	0.29
32	4.20 ± 0.01	−0.72 ± 0.01	1.00	0.13	4.67 ± 0.01	−0.63 ± 0.04	0.99	0.12
33.3	4.17 ± 0.01	−0.70 ± 0.02	1.00	0.19	4.66 ± 0.01	−0.74 ± 0.03	0.98	0.13
35	4.49 ± 0.01	−0.76 ± 0.04	1.00	0.45	4.84 ± 0.02	−0.67 ± 0.03	1.00	0.45
	PC:PE:PI:CHO:ATPase-FITC				PC:PE:PI:CHO:ATPase-IAF			
[CHO] (mol %)	τ_u (ns)	β	f_i	χ^2	τ_u (ns)	β	f_i	χ^2
22	4.42 ± 0.01	−0.68 ± 0.01	0.99	0.15	4.77 ± 0.01	−0.72 ± 0.02	0.97	0.20
24	4.38 ± 0.01	−0.64 ± 0.02	0.99	0.10	4.64 ± 0.01	−0.69 ± 0.01	0.97	0.14
25	4.39 ± 0.01	−0.68 ± 0.03	1.00	0.16	4.70 ± 0.01	−0.70 ± 0.01	0.97	0.13
26	4.44 ± 0.01	−0.69 ± 0.03	0.99	0.13	4.82 ± 0.01	−0.72 ± 0.02	0.97	0.15
27	4.41 ± 0.01	−0.69 ± 0.03	0.99	0.18	4.64 ± 0.01	−0.72 ± 0.02	0.97	0.33
29	4.47 ± 0.01	−0.62 ± 0.02	0.98	0.17	4.74 ± 0.01	−0.71 ± 0.01	0.97	0.17
32	4.45 ± 0.01	−0.63 ± 0.02	0.99	0.15	4.73 ± 0.01	−0.67 ± 0.02	0.97	0.25
33.3	4.45 ± 0.01	−0.63 ± 0.01	0.98	0.13	4.71 ± 0.01	−0.70 ± 0.01	0.97	0.17
35	4.49 ± 0.01	−0.70 ± 0.03	0.98	0.22	5.02 ± 0.02	−0.65 ± 0.05	0.97	0.25

[a] τ_u and τ_L refer to the upper and lower limits of the asymmetric distribution of lifetimes. β refers to the density-of-state parameter describing the distribution of lifetimes between the two limits. f_i corresponds to the fractional contribution to the intensity of the upper limit. During the analysis all parameters were permitted to float, though, in all cases the recovered value for τ_L was between 0.18 and 0.22. The reduced chi-square (χ^2) value corresponds to the fit of the phase and modulation data to the model. The errors given in parentheses represent the correlated 67% confidence limits of the reduced χ^2.

Table 4: Anisotropy Decay Parameters of Fluorescein-Labeled Pig Kidney Na^+/K^+-ATPase Reconstituted in Natural Lipid Unilamelar Vesicles, Effect of Modification of Membrane Cholesterol Content, and Phase and Modulation Data Analyzed according to a Two-Exponential Decay Model[a]

	PC:CHO:ATPase-FITC					PC:CHO:ATPase-IAF				
[CHO] (mol %)	r_0	f_{xb}	ϕ_F (ns)	ϕ_S (ns)	χ^2	r_0	f_{xb}	ϕ_F (ns)	ϕ_S (ns)	χ^2
22	0.30	0.20 ± 0.03	1.22 ± 0.02	82 ± 6	0.37	0.30	0.21 ± 0.01	1.03 ± 0.07	87 ± 7	0.15
24	0.31	0.17 ± 0.02	1.42 ± 0.08	110 ± 3	0.10	0.30	0.21 ± 0.01	1.46 ± 0.07	117 ± 4	0.18
25	0.32	0.15 ± 0.01	1.29 ± 0.03	102 ± 8	0.20	0.30	0.21 ± 0.01	1.20 ± 0.09	103 ± 10	0.12
26	0.31	0.15 ± 0.01	1.19 ± 0.03	90 ± 3	0.18	0.28	0.22 ± 0.01	1.04 ± 0.01	104 ± 11	0.14
27	0.31	0.16 ± 0.01	1.45 ± 0.05	100 ± 20	0.15	0.30	0.21 ± 0.01	1.40 ± 0.09	114 ± 10	0.29
29	0.32	0.17 ± 0.01	1.40 ± 0.05	95 ± 15	0.12	0.31	0.22 ± 0.01	1.26 ± 0.06	100 ± 16	0.23
32	0.32	0.17 ± 0.01	1.22 ± 0.04	85 ± 10	0.13	0.30	0.22 ± 0.01	1.31 ± 0.06	121 ± 14	0.33
33.3	0.31	0.17 ± 0.02	1.16 ± 0.04	120 ± 9	0.16	0.31	0.22 ± 0.01	0.97 ± 0.09	86 ± 12	0.16
35	0.32	0.19 ± 0.01	1.37 ± 0.05	106 ± 8	0.14	0.30	0.22 ± 0.01	1.37 ± 0.07	122 ± 23	0.10
	PC:PE:PI:CHO:ATPase-FITC					PC:PE:PI:CHOL:ATPase-IAF				
[CHO] (mol %)	r_0	f_{xb}	ϕ_F (ns)	ϕ_S (ns)	χ^2	r_0	f_{xb}	ϕ_F (ns)	ϕ_S (ns)	χ^2
22	0.29	0.20 ± 0.03	1.40 ± 0.05	86 ± 6	0.16	0.27	0.25 ± 0.01	1.45 ± 0.05	105 ± 5	0.37
24	0.31	0.19 ± 0.02	1.11 ± 0.06	80 ± 5	0.13	0.29	0.25 ± 0.02	1.30 ± 0.03	93 ± 4	0.31
25	0.30	0.18 ± 0.01	1.15 ± 0.05	77 ± 7	0.18	0.29	0.24 ± 0.01	1.45 ± 0.05	95 ± 12	0.24
26	0.31	0.20 ± 0.01	1.49 ± 0.07	102 ± 9	0.10	0.27	0.26 ± 0.01	1.65 ± 0.05	85 ± 15	0.25
27	0.31	0.19 ± 0.01	1.45 ± 0.06	88 ± 7	0.10	0.28	0.26 ± 0.01	1.54 ± 0.03	68 ± 8	0.24
29	0.31	0.20 ± 0.01	1.48 ± 0.05	98 ± 10	0.10	0.28	0.25 ± 0.01	1.40 ± 0.03	75 ± 4	0.23
32	0.31	0.20 ± 0.01	1.55 ± 0.08	113 ± 11	0.15	0.26	0.25 ± 0.01	1.35 ± 0.02	126 ± 34	0.44
33.3	0.30	0.20 ± 0.01	1.43 ± 0.04	115 ± 8	0.10	0.27	0.25 ± 0.01	1.24 ± 0.03	85 ± 5	0.27
35	0.31	0.20 ± 0.01	1.52 ± 0.04	100 ± 13	0.15	0.28	0.24 ± 0.01	1.35 ± 0.02	96 ± 10	0.21

[a] r_0 refers to the time 0 anisotropy. f_{xb} refers to the fraction of the observed anisotropy decay associated with the fast depolartization process. ϕ_F and ϕ_S refer to the fast and slow rotational correlation times. The reduced chi-square (χ^2) value corresponds to the fit of the phase and modulation data to the model., The errors given in parentheses represent the correlated 67% confidence limits of the reduced χ^2. r_0 errors were all 0.01.

hindered rotator model were slightly different, the results also showed dips for ϕ_F at these same cholesterol concentrations (data not shown).

FTIR-ATR Measurements. The effect of membrane cholesterol content on the lipid phase and on the enzyme properties was also studied by IR spectroscopy using the FTIR-ATR technique. Spectra were obtained from samples consisting of planar bilayers supported on an ATR germanium plate with D_2O phosphate buffer at 37 °C (see Materials and Methods). The symmetric and antisymmetric methylenic C—H stretching (2800−3000 cm^{-1}) and C═O stretching (1700−1760 cm^{-1}) lipid bands and the protein amide I band

Table 5: Ratio of Areas of the Deconvoluted Components of the Lipid C═O Vibrational Band in Unilamellar Vesicles with Reconstituted Pig Kidney Na^+/K^+-ATPase and Effect of Modification of Membrane Cholesterol Content[a]

	A_{1726}/A_{1742}	
[CHO] (mol %)	PC:CHO:ATPase	PC:PE:PI:CHO:ATPase
22	1.0 ± 0.1	5.3 ± 2.1
24	1.7 ± 0.1	1.0 ± 0.6
25	0.9 ± 0.1	1.3 ± 0.8
26	0.4 ± 0.1	2.8 ± 0.7
27	0.8 ± 0.2	2.1 ± 0.2
29	0.8 ± 0.2	4.2 ± 0.2
32	0.3 ± 0.1	2.2 ± 0.3
33.3	0.2 ± 0.1	1.0 ± 0.8
35	1.1 ± 0.1	1.3 ± 0.7

[a] A_{1726}/A_{1742} refers to the ratio of the areas of the resolved components with peaks located at 1726 and 1742 cm^{-1}, respectively. Each point represents an average of data in duplicate and standard error.

(1600−1700 cm^{-1}) were analyzed. The C═O vibrational band was deconvoluted, using Lorentzian distributions, into two components with peaks at 1726 and 1743 cm^{-1} corresponding to the two well-established populations of carbonyl groups in a lipid bilayer associated with those hydrogen bonded to water and free groups, respectively (*61*, *62*). In this regard, the effect of modification of the cholesterol content was assessed through the ratio of the areas of both deconvoluted components (A_{1726}/A_{1743}), shown in Table 5 , where abrupt changes were observed that showed dips at 24 and 33.3 cholesterol mol % for PC:PE:PI vesicles and at 26 and 33.3 mol % for PC vesicles, though the second dip of the first system was not significant with respect to the last value.

The antisymmetric C−H stretching band observed at 2927 cm^{-1} did not show significant spectral shifts with modification of the cholesterol content. The symmetric band observed at 2854 cm^{-1} showed a slight shift to lower frequencies as cholesterol was increased. This effect has been related to a reduction of lipid chain trans-gauche rotamers. Considerable band shape changes and spectral shifts of the protein amide I band were apparent upon modification of the membrane cholesterol content. Figure 2 shows the amide I band maximum as a function of membrane cholesterol content. A nonmonotonic spectral shift of the maximum was observed, with biphasic variations showing two peaks at 24 and 33.3 cholesterol mol % for PC:PE:PI:CHO:ATPase vesicles and at 25 and 33.3 mol % for PC:CHO:ATPase vesicles. These patterns were coincident with the peaks or dips observed for the enzymatic activity and for the bilayer and protein properties, considered in this work, with the exception of the peak at 25 mol % for PC vesicles which was exactly at the critical cholesterol concentration predicted by the regular distribution model (*20*−*23*). The amide I band was deconvoluted with a method considering mixed Lorentzian and Gaussian components. The best fits, according to χ^2 values, were obtained with nine curves with a bandwidth at half-height of 7.5. The position and areas of the curves were permitted to float. α-Helix, β-sheet, turns, and random coil contributions to the secondary structure were calculated, according to the assignment of Jackson and Mantsch (*63*), which are shown in Table 6 for vesicles with different cholesterol content. No trend was found in the variation of the secondary structure with modification of the cholesterol content; interestingly, however, the states corresponding to 24 and 33.3 cholesterol mol % for PC:PE:PI vesicles and to 26 and 33.3 mol % for PC vesicles were the only pair of states in each table that showed no significant differences between them in all four secondary structures.

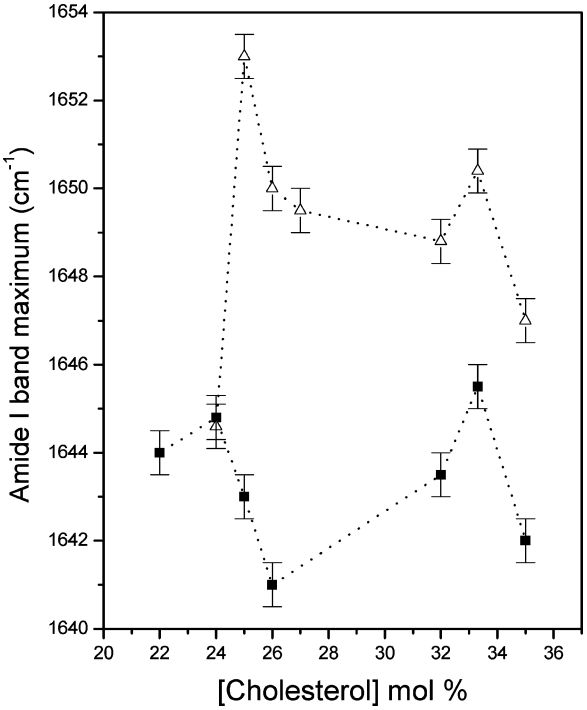

FIGURE 2: FTIR-ATR, amide I band maximum of Na^+/K^+-ATPase reconstituted in unilamellar vesicles of natural lipids, as a function of membrane cholesterol content, at 37 °C. Each point represents an average of data in duplicate and standard error. Key: (△) PC:PE:PI:CHO vesicles; (■) PC:CHO vesicles.

DISCUSSION

In this study, the effects of membrane cholesterol content on Na^+/K^+-ATPase activity and on membrane and protein properties were investigated. These studies were achieved by reconstituting purified enzyme into unilamellar vesicles of natural lipid of defined composition wherein cholesterol content was modified. The cholesterol concentration interval studied, between 22 and 35 mol %, includes two critical cholesterol concentrations, 25 and 33.3 mol %, predicted by the superlattice or regular distribution model (*20*−*23*).

Utilizing a reconstitution process that allows the proper equilibration of lipids and protein molecules, we were able to obtain unilamellar vesicles with the reconstituted Na^+/K^+-ATPase in an oriented membrane in which the enzyme constitutes a major fraction (95%) of the membrane protein without loss of ATPase activity (see Results). In both types of natural lipid vesicles considered in this work, PC:PE:PI:CHO and PC:CHO, the reconstituted enzyme showed, in general, a higher activity than in the native membrane preparation. In this regard, Cornelius (*34*) maintained that a fluid membrane with a PC chain length of about 18 and cholesterol is sufficient to support optimal Na^+/K^+-ATPase activity. Our results, referred to natural lipids, indicate that although a membrane with natural PC and cholesterol is adequate to sustain a high ATPase activity, the enzyme reconstituted in vesicles of a mixture of natural PC:PE:PI:CHO, mimicking a natural membrane, showed a significant

Table 6: Secondary Structures of Pig Kidney Na^+/K^+-ATPase Reconstituted in Natural Lipid Unilamellar Vesicles and Supported Planar Bilayer on the ATR Germanium Plate and Effect of Modification of Membrane Cholesterol Content[a]

	PC:CHO:ATPase				PC:PE:PI:CHO:ATPase			
[CHO] (mol %)	turns	α-helix	random coil	β-sheet	turns	α-helix	random coil	β-sheet
22	31.4 ± 1.4	24.9 ± 1.9	9.3 ± 1.6	34.4 ± 0.5	15.9 ± 0.4	18.5 ± 0.9	11.4 ± 0.6	54.8 ± 1.5
24	20.3 ± 0.6	49.2 ± 2.2	12.7 ± 0.6	17.8 ± 1.1	21.5 ± 0.4	23.1 ± 2.2	20.0 ± 0.3	35.4 ± 2.1
25	32.6 ± 0.9	21.3 ± 1.5	16.8 ± 1.0	29.3 ± 2.1	22.6 ± 1.9	25.2 ± 0.5	19.4 ± 1.8	32.9 ± 2.1
26	36.6 ± 0.7	21.7 ± 0.7	16.2 ± 1.1	25.5 ± 0.7	22.9 ± 0.9	15.4 ± 0.9	14.0 ± 0.1	47.9 ± 0.1
27	30.0 ± 0.5	25.0 ± 0.9	15.0 ± 1.4	30.0 ± 0.8	18.5 ± 1.5	21.2 ± 0.6	18.1 ± 2.4	42.3 ± 0.3
29	29.0 ± 1.2	26.0 ± 1.2	14.0 ± 0.8	31.0 ± 1.0	14.0 ± 0.2	21.1 ± 0.2	18.0 ± 1.4	46.9 ± 1.0
32	36.1 ± 0.8	22.4 ± 1.6	12.7 ± 0.7	28.8 ± 1.4	25.7 ± 0.2	24.9 ± 1.9	12.1 ± 1.7	32.3 ± 0.4
33.3	37.5 ± 0.7	21.4 ± 1.5	15.1 ± 1.4	26.0 ± 0.9	21.1 ± 0.3	20.9 ± 2.5	20.4 ± 2.4	37.6 ± 0.2
35	31.4 ± 1.4	24.9 ± 1.9	9.3 ± 1.6	34.4 ± 0.5	18.5 ± 1.8	20.6 ± 0.6	27.2 ± 1.4	33.7 ± 2.6

[a] Data from the FTIR-ATR amide I band were analyzed with mixed Lorentzian and Gaussian components.

higher activity than in the former (Figure 1). Our results, however, are difficult to compare directly with those of Cornelius (*34*) since different enzyme sources were used. What is most significant about the results reported here is that the response of the enzymatic activity to modification of the cholesterol content revealed abrupt changes with significant peaks at 24 and 33.3 cholesterol mol % for PC:PE:PI:CHO vesicles and at 26 and 33.3 mol % for PC:CHO vesicles. Notably, these peaks were located at or near the critical cholesterol concentrations mentioned above. This effect was examined in groups of samples that had the same amount of enzyme and substrate (ATP) so that the cholesterol mole fraction was the only difference between samples. In this context, the result that small changes in membrane cholesterol content caused significant changes in enzymatic activity (up to 37%) in the two narrow regions of the cholesterol interval considered in this work can only be ascribed to composition-dependent changes in membrane organization. Several lines of evidence indicate that conformational changes occur in Na^+/K^+-ATPase during the catalytic cycle. These changes affect the enzyme's affinity for its ligands, cause a reorientation of bound ATP necessary for its hydrolysis, and accomplish occlusion and translocation of Na^+ and K^+ across the cell membrane. However, the nature of the conformational changes that have been postulated remains largely a matter of speculation. In order to obtain experimental evidence regarding concomitant membrane organization and protein changes relating to the role of cholesterol in modulating the enzyme's activity, we also investigated the response of fluorescent membrane probes, enzyme-linked fluorescein probes, and probe-free FTIR parameters. In this context, the membrane probe Laurdan was used to search for hydration and/or molecular dynamics changes at the level of the phospholipid glycerol backbone region, the so-called hydrophilic−hydrophobic interface of the membrane. With its lauric acid tail anchored in the phospholipid acyl chain region and the fluorescent naphthalene moiety at the hydrophilic−hydrophobic interface, its fluorescence spectrum is highly sensitive to the polarity and dynamics of the environment of its fluorescent moiety due to its large excited-state dipole (*64*). Consequently, Laurdan presents large spectral shifts upon changes in the properties of the environment, specifically to the concentration and/or to the relaxation properties of water molecules present at the hydrophobic−hydrophilic interface (*65*). Using the general polarization parameter GP to quantify Laurdan's fluorescence spectral shifts, we found that its fluorescence spectrum presented significant spectral shifts when membrane cholesterol content was modified. The general trend of GP increase with cholesterol content increase found in both types of vesicles without protein was consistent with the reported effect of cholesterol decreasing both hydration and molecular dynamics at this interface (*66*). However, a different behavior was found in vesicles with the reconstituted enzyme; namely, cholesterol increase induced a slight GP decrease in PC:PE:PI:CHO vesicles, while in PC:CHO vesicles no significant change was apparent up to 32 cholesterol mol %, followed by a pronounced GP increase at the two higher cholesterol concentrations. These results indicate that the phospholipid composition, with regard to its polar head groups, affects the physicochemical properties of the bilayer at this level. Thus, the PC:PE:PI:CHO membrane showed higher GP values than PC:CHO membranes; moreover, enzyme reconstitution induced a decrease in GP in the latter but not in the former system. Spectral shift, i.e., GP value, depends on the extent of solvent relaxation; in a membrane, water content as well as the neighboring lipid polar groups can affect solvent relaxation around the fluorophore, and in the case of the PC:PE:PI:CHO membrane, the inositol group on PI may restrict water relaxation, thus producing a higher GP. We propose that the effect of the inositol group could be responsible for the different behavior of the PC:PE:PI:CHO membrane with respect to the PC:CHO membrane when the enzyme is reconstituted. Nonetheless, the most significant aspect of the Laurdan results is that the effect of membrane cholesterol content modification on GP values was not monotonic but rather that abrupt changes occurred that were coincident with the peaks in the enzymatic activity. Notably, these peaks corresponded to states of slightly lower hydration and/or molecular dynamics of the membrane at this shallow depth.

We also used the membrane probe DPH to examine the hydrophobic membrane core. The lifetime data were analyzed in the context of continuous distributions in order to account for the environmental heterogeneity. Since DPH lifetime is extremely sensitive to the environment dielectric constant (*67*), the general trend of DPH lifetime increase with membrane cholesterol content was interpreted as due to the effect of cholesterol in decreasing the interchain hydration (*37*). A concomitant cholesterol ordering effect in this membrane domain was also inferred from a general trend of DPH steady-state fluorescence anisotropy increase found in the same cholesterol content interval (data not shown). The latter effect has also been postulated from theoretical developments (*68*). Interestingly, although both vesicles showed similar DPH lifetime values in the absence of the

enzyme, its inclusion had a different effect in each system. In the PC:PE:PI:CHO membrane, enzyme reconstitution induced a slight decrease in the lifetime, indicating a corresponding lipid phase hydration increase at the hydrophobic membrane core. The opposite effect was found in the PC:CHO membrane. These results suggest that the polar headgroups of the phospholipids could also have an effect in the hydrophobic bilayer region, possibly due to specific lipid−protein interactions. Notably, modification of the cholesterol content also induced a nonmonotonic response in the DPH lifetime. In both types of membranes without the enzyme, abrupt changes in the lifetime occurred at the same cholesterol contents where enzyme activity peaks were found, i.e., 24 and 33.3 mol % in PC:PE:PI:CHO membranes and 26 and 33.3 mol % in PC:CHO membranes. This result indicates that these states have slight but significant lower hydration. In membranes with the reconstituted enzyme abrupt changes were also noticeable; however, in PC:PE:PI:CHO membranes the peak at 24 mol % was not a significant increment. In PC:CHO membranes, on the other hand, 26 and 33.3 mol % correspond to slope changes after considerable lifetime increments.

Results of both membrane probes, Laurdan and DPH, indicated that the lipid phase of the membrane states, at or near the two critical cholesterol concentrations predicted by the superlattice theory, presented slightly lower hydration at the glycerol backbone level and at the hydrophobic interchain domain. In both systems, these states were those that presented the highest enzymatic activity.

Two enzyme domains were studied investigating the fluorescence emission decay and the fluorescence anisotropy decay of fluorescein conjugated to a lysine and cysteine enzyme residues through FITC and IAF labeling, respectively. As the labeling procedures were done prior to the solubilization and reconstitution steps, i.e., the enzyme bound to membrane fragments or to open/leaky vesicles, the cytosolic and extracellular protein domains were exposed to the reagents. In the first case, the 1:1 probe:protein ratio, FITC labeling is proposed to occur at a lysine residue of the main cytosolic protein domain, at or near the ATP active site. Indeed, our results indicated total inactivation of the ATPase activity of the labeled enzyme as well as a protective effect of ATP to FITC labeling, in accordance with previous findings (*47*, *69*, *70*). IAF labeling, in a 3:1 probe:protein ratio, however, did not produce a significant loss of ATPasic activity, was independent of ATP presence, and occurred only in the presence of potassium ion, in accordance with previous findings (*48*, *60*, *71*). These findings indicated that IAF labeling sites are somewhat removed from the ATP active site. Different cysteine residues have been proposed to be available, in certain conditions, for IAF labeling such as Cys 457 located in the main cytoplasmic domain (between transmembrane segments H4−H5) and Cys 802, 964, and 911 in transmembrane domains close to the extracellular membrane−aqueous border (*60*, *72*−*74*). Considering the conditions of our labeling and those in the references listed, we consider that in our system all or at least two of the labeled cysteines correspond to cytoplasmic domains, but we cannot rule out, in the pig kidney enzyme, labeling of another cysteine at or close to the extracellular membrane aqueous border, although we consider this case to be less probable.

Fluorescein emission decay was analyzed with the asymmetric distribution model of Alcala et al. (*52*), according with Klonis and Sawyer (*55*), as a proper model for a fluorescein-labeled protein (see Results). The upper lifetime distribution limit, τ_u, has been used as the parameter of interest for the discussion. These authors have also indicated that the decrease in the polarity of the environment increases the monoanion contribution to the measured absorbance and fluorescence and that, unlike the quantum yield and lifetime of the dianion, the corresponding parameters of the monoanion are sensitive to the environment surrounding the fluorophore, with a general increase of the monoanion quantum yield and lifetime, in environments with less water (*75*, *76*). In this context, the rather high lifetime values obtained for both types of labeling suggest that the modified lysine and cysteines were in environments fairly well protected from water, particularly the modified cysteines showing higher lifetime values at all of the cholesterol concentrations. Interestingly, the abrupt changes in fluorescein lifetimes with cholesterol content modification, with slight but significant dips, coincident with the states of enzyme activity peaks, i.e., 24 and 33.3 mol % in PC:PE:PI:CHO membranes and 26 and 33.3 mol % in PC:CHO membranes, suggest that a slight but significant hydration increase occurred in the examined protein domains at these critical cholesterol concentrations. This hydration increase would be concomitant with the corresponding lipid phase hydration decrease, as discussed above.

FITC- and IAF-labeled enzymes were also used in conjunction with time-resolved fluorescence anisotropy to assess peptide backbone flexibility and rapid molecular motions in Na^+/K^+-ATPase. For this purpose, we investigated the fluorescence anisotropy decay of the fluorescein-modified lysine and cysteine residues as function of membrane cholesterol content. Time-resolved fluorescence anisotropy permits one to examine the reorientation of fluorophore molecules in a time domain of several excited-state lifetimes. When a fluorophore is conjugated to peptidyl side chains, as in the present case, the motion of the fluorophore and hence the depolarization are achieved by multiple relaxation processes in different time frames. Very fast rotations around the tethered arm can occur, if unhindered, in a subnanosecond time window and are thus unresolvable with our instrumentation. These types of fast motions are, however, reflected by the time zero anisotropy values (r_0) with an amplitude of ($r_i - r_0$), where r_i corresponds to the fundamental anisotropy of the fluorophore (*77*). On the other hand, small-scale peptidyl segmental motions of protein segments bearing the fluorophore should give rise to fast depolarizations, in the low nanosecond time frame, characterized by an amplitude, $r_0 f_{xb}$, and a rotational correlation time, ϕ_F. The macromolecule whole-body rotational diffusion is responsible for the slowest rate of anisotropy decay, related with a ϕ_S. Results (Table 4) showed similar values for the slow rotational correlation time of both types of labeled residues and for both types of vesicles, in a range of values considered to be physically meaningless due to the low ratio of the lifetime to the rotational correlation time (see Results). As a general trend for all cholesterol concentrations, the values obtained for the rotational correlation time of the fast anisotropy decay component, ϕ_F (between 0.97 and 1,65 ns), indicated a significant level of

backbone flexibility around all labeled sites. Likewise, the amplitudes of the very fast ($r_i - r_0$) and fast decay processes ($r_0 f_{xb}$) represented a slightly higher percentage of the total anisotropy decay when fluorescein is conjugated to cysteine residues than to lysine residues, and in both cases this percentage was higher when the enzyme was reconstituted in PC:PE:PI:CHO than in PC:CHO vesicles. As these amplitudes are related to fluorescein motion around its tether arm and flexible backbone segmental motions of the protein-examined domains, respectively, these differences suggested a lower degree of hindrance for both types of motions around the labeled cysteines and also around both types of residues when the enzyme was embedded in PC:PE:PI:CHO membrane. However, the most interesting results for this discussion are that modification of the membrane cholesterol content induced nonmonotonic abrupt changes in the fast rotational correlation time, giving rise to slight but significant dips in this parameter at the same critical cholesterol concentrations where dips of fluorescein lifetime and peaks in the ATPase activity were apparent, i.e., 24 and 33.3 mol % in PC:PE:PI:CHO membranes and 26 and 33.3 mol % in PC:CHO membranes. These results indicated that peptide backbone segmental motions of the protein, at least around the labeled residues, presented slight but significantly faster dynamic flexibility at these critical membrane cholesterol concentrations.

The biochemical activity of a protein strictly depends on its conformation because the functions of all proteins rely on the precise spatial positioning of several functional groups with respect to each other (*78*). Thus, an understanding of a membrane protein structure and its changes is crucial for elucidating the enzyme mechanism. In this respect there is increasing agreement about the importance of the environment as well as the amino acid sequence in determining the secondary structure of a protein (*79*, *80*). For membrane-associated proteins the interactions with the lipid phase are considered to play a key role in shaping its conformation. Along these lines, a vast majority of the membrane proteins whose X-ray structures are known have their transmembrane sequences in α-helical conformations, showing a remarkable similarity in their main infrared amide I band maximum frequency, consistent with this conformation (*81*). In this context we used Fourier transform infrared spectroscopy, with the attenuated total reflectance technique (ATR-FTIR), to examine possible enzyme structural changes associated with membrane cholesterol modification. IR spectra were obtained in the same membranes used previously, i.e., PC:CHO:ATPase and PC:PE:PI:CHO:ATPase, but as supported planar bilayers on an ATR germanium plate, which were obtained from the corresponding vesicles with the reconstituted enzyme (see Materials and Methods). The medium above the ATR plate in all cases was D_2O phosphate buffer. We analyzed the amide I band, observed in the region 1600−1700 cm^{-1}, as it is the most useful for protein secondary structure analysis. In our samples, at 37 °C, the maxima of this band for PC:CHO bilayers were observed in the interval 1645−1653 cm^{-1} and in the interval 1641−1646 cm^{-1} for PC:PE:PI:CHO bilayers. Importantly, the amide I band maximum showed a temperature dependence in our systems; thus, in the PC:CHO:ATPase system with a cholesterol concentration of 25 mol % the absorption maximum was shifted from 1653 to 1657 cm^{-1} when the temperature was lowered from 37 to 20 °C (data not shown); the value at 20 °C was consistent with previous findings (*81*). Such an absorption is considered to be characteristic of a protein containing α-helical polypeptide segments (ref *82* and references cited therein).

Notably, the amide I band maximum showed spectral shifts, in both types of membranes, with cholesterol content modification, inducing a nonmonotonic frequency variation pattern (Figure 2). Peaks are apparent at or near the critical cholesterol concentrations considered in this work, i.e., at 25 and 33.3 mol %, where the enzyme showed the highest activity. One explanation for this effect is that conformational changes occur when membrane cholesterol content is modified. Therefore, quantitative analysis of the enzyme secondary structure was undertaken in order to assess the effect of cholesterol concentration upon protein structure. The corresponding results (Table 6) indicated, for both type of membranes, that no definite variation trends on the secondary structure were apparent with membrane cholesterol content modification. α-Helix and β-sheet contributions were within the interval of previous findings (*83*, *84*). These results suggest that the spectral shifts of the amide I band maximum in the infrared spectrum cannot therefore be attributed to secondary structure changes with membrane cholesterol content. Another explanation arises from the proposal that the absorption of α-helical structure in D_2O is sensitive to the degree of solvent interaction, with a decrease in amide I frequency when the hydration increases (*82*). If this were the case, these nonmonotonic frequency variations suggest that changes in the interactions of the enzyme transmembrane domains with solvent would occur, due to cholesterol-induced membrane hydration modifications, with two states of lowest hydration at the observed peaks. This explanation is in agreement with our hypothesis, mentioned above, postulating that the lipid phase presented slight lower hydration at the glycerol backbone level and at the hydrophobic interchain domains in both states with critical cholesterol concentrations. Also in this context, the lower frequency interval observed for amide I band maxima in PC:PE:PI:CHO bilayers (1641−1646 cm^{-1}) than in PC:CHO bilayers (1645−1653 cm^{-1}) would indicate that bilayer hydration was higher in the former than in the latter.

As already stated, the results of the enzyme secondary structure analysis revealed, in both types of membranes, variations in all four components, when cholesterol content was modified, but these variations did not reveal any trends (Table 6). Manifestly, however, for each type of membrane, the two compositions that showed the highest ATPase activity, i.e., at or near the critical cholesterol concentrations, the overall enzyme secondary structure appeared to be the same. No other pair of states, for each type of vesicles (26 and 33.3 cholesterol mol % in one case and 24 and 33.3 cholesterol mol % in the other case), has the same contribution in all four of the components considered, within the limits of the corresponding standard errors. These results, combined with those mentioned above, suggest that a relation might exist between the bilayer organization and the enzyme structural/dynamics characteristics, therefore influencing its activity. On the other hand, they also suggest that the structural and dynamical changes that occur both in the lipid phase and in the enzyme, concomitant with the enzyme ATPase activity changes, consist of small variations of the

corresponding properties. Therefore, it seems probable that the enzyme activity increase at the critical cholesterol concentrations could be the result of a combination of small protein structural and dynamical changes induced by these small composition-dependent changes in the membrane organization as it evolves toward a superlattice organization. In this regard, Chetverin et al. indicated that according to their results the enzyme working cycle lacks gross structure changes (*85*). On the other hand, Pratap et al., reporting an investigation related to ATP-induced conformational changes in Na^+/K^+-ATPase, indicated that from their FTIR results it is not possible to decide if these changes correspond to large changes localized in the cytoplasmic loop between the M4 and M5 transmembrane domains or a sum of smaller changes that occurred throughout the protein (*86*).

We consider that this behavior can be explained in the context of the membrane superlattice or regular distribution model (*20*−*22*), according to which cholesterol molecules tend to be regularly distributed in a hexagonal host lipid lattice; however, irregular distributions always coexist with regular distributions, resulting in segregated domains. On the other hand, different experimental evidence suggested that these domains may have very small/submicroscopic dimensions (*14*, *28*, *29*). Since, according to this model, the ratio of regular to irregular regions reaches local maxima at critical cholesterol mole fractions, we suggest that at these states the domain boundary surfaces also reach local maxima. Therefore, it seems likely that at the two critical cholesterol concentrations, examined in this work, the reconstituted Na^+/K^+-ATPase might be further associated with these boundaries. Moreover, in this regard, Cannon et al. (*32*) presented compelling evidence that proteins tend to migrate to domain boundaries, in the context of the depletion-potential model, although, according to the authors, further experiments are needed to substantiate such propositions. In this sense, important evidence related to enhanced protein activities in environments with segregated domains has been reported (*24*, *32*, *87*−*89*). The explanation for these enhancements rests on the proposition that boundaries are sites of structural irregularities and defects where the lipids should be more loosely packed, allowing the protein less hindered dynamics than in a homogeneous environment (*32*).

In this context, we consider that local motions of the polypeptide chain would be the most favored ones at the critical cholesterol concentrations. The dips observed in the fast rotational correlation time could be related to this effect. However, this conclusion would imply that changes in transmembrane segments could be transmitted to cytoplasmic domains. This type of effect has been previously suggested for this enzyme, e.g., the modification of an extracellular ouabain site upon a cytoplasmatic domain 5-IAF binding (*58*).

CONCLUDING REMARKS

We propose that composition-dependent superlattice formation in membranes has important implications for the regulation of Na^+/K^+-ATPase activity. Taken together, the results presented here indicate that when the lipid phase is in the vicinity of a critical mole fraction, for superlattice formation, minute changes in its cholesterol concentration produce abrupt changes in the membrane organization. These changes, in turn, induce small changes in the protein's structure and dynamics, therefore acting to fine-tune the enzyme by sorting it into membrane interdomain boundaries. Importantly, superlattice states correspond to free energy local minima (*22*, *24*), suggesting that their formation should be a thermodynamically driven process and, hence, may occur in natural membranes.

ACKNOWLEDGMENT

Time-resolved experiments reported in this paper were performed at the Laboratory for Fluorescence Dynamics (LFD) at the University of Illinois at Urbana−Champaign (UIUC). The LFD is supported jointly by the National Center for Research Resources of the National Institutes of Health (PHS 5 P41-RR003155) and UIUC. We thank Dr. Susana Sanchez for assistance with the time-resolved measurements at the LFD.

REFERENCES

1. Jorgensen, P. L. (1985) Molecular basis for active Na, K-transport by Na^+/K^+-ATPase from outer renal medulla, *Biochem. Soc. Symp. 50*, 59−79.
2. Kaplan, J. H. (2002) Biochemistry of Na^+/K^+-ATPase, *Annu. Rev. Biochem. 71*, 511−535.
3. Wuddel, I., and Apell, H. J. (1995) Electrogenicity of the sodium transport pathway in the Na^+/K^+-ATPase probed by charge-pulse experiments, *Biophys. J. 69*, 909−921.
4. Yeagle, P. L., Young, J., and Rice, D. (1988) Effects of cholesterol on Na^+/K^+-ATPase ATP hydrolyzing activity in bovine kidney, *Biochemistry 27*, 6449−6452.
5. Sutherland, E., Dixon, B. S., Leffert, H. L., Skally, H., Zaccaro, L., and Simon, F. R. (1988) Biochemical localization of hepatic surface-membrane Na^+/K^+-ATPase activity depends on membrane lipid fluidity, *Proc. Natl. Acad. Sci. U.S.A. 85*, 8673−8677.
6. Cornelius, F. (1991) Functional reconstitution of the sodium pump. Kinetics of exchange reactions performed by reconstituted Na^+/K^+-ATPase, *Biochim. Biophys. Acta 1071*, 19−66.
7. Chong, P. L., Fortes, P. A., and Jameson, D. M. (1985) Mechanisms of inhibition of Na^+/K^+-ATPase by hydrostatic pressure studied with fluorescent probes, *J. Biol. Chem. 260*, 14484−14490.
8. Sinensky, M., Pinkerton, F., Sutherland, E., and Simon, F. R. (1979) Rate limitation of Na^+/K^+-stimulated adenosinetriphosphatase by membrane acyl chain ordering, *Proc. Natl. Acad. Sci. U.S.A. 76*, 4893−4897.
9. Jacobson, K., Sheets, E. D., and Simson, R. (1995) Revisiting the fluid mosaic model of membranes, *Science 268*, 1441−1442.
10. Parassasi, T., and Gratton, E. (1995) Membrane lipid domains and dynamics as detected by Laurdan fluorescence, *J. Fluoresc. 5*, 59−68.
11. Simons, K., and Ikonen, E. (1997) Functional rafts in cell membranes, *Nature 387*, 569−572.
12. Edidin, M. (2003) Lipids on the frontier: a century of cell-membrane bilayers, *Nat. Rev. Mol. Cell Biol. 4*, 414−418.
13. Brown, D. A., and London, E. (2000) Structure and function of sphingolipid- and cholesterol-rich membrane rafts, *J. Biol. Chem. 275*, 17221−17224.
14. Silvius, J. R. (2003) Fluorescence energy transfer reveals microdomain formation at physiological temperatures in lipid mixtures modeling the outer leaflet of the plasma membrane, *Biophys. J. 85*, 1034−1045.
15. Ipsen, J. H., Karlstrom, G., Mouritsen, O. G., Wennerstrom, H., and Zuckermann, M. J. (1987) Phase equilibria in the phosphatidylcholine-cholesterol system, *Biochim. Biophys. Acta 905*, 162−172.
16. Nielsen, M., Miao, L., Ipsen, J. H., Zuckermann, M. J., and Mouritsen, O. G. (1999) Off-lattice model for the phase behavior of lipid-cholesterol bilayers, *Phys. Rev. E: Stat. Phys., Plasmas, Fluids, Relat. Interdiscip. Top. 59*, 5790−5803.
17. Nielsen, M., Miao, L., Ipsen, J. H., Zuckermann, M., and Mouritsen, O. G. (1999) Off-lattice model for the phase behavior of lipid-cholesterol bilayers, *Phys. Rev. E 59*, 5790−5803.

18. Sankaram, M. B., and Thompson, T. E. (1991) Cholesterol-induced fluid-phase immiscibility in membranes, *Proc. Natl. Acad. Sci. U.S.A. 88*, 8686−8690.
19. Parasassi, T., Giusti, A. M., Raimondi, M., and Gratton, E. (1995) Abrupt modifications of phospholipid bilayer properties at critical cholesterol concentrations, *Biophys. J. 68*, 1895−1902.
20. Somerharju, P. J., Virtanen, J. A., Eklund, K. K., Vainio, P., and Kinnunen, P. K. J. (1985) 1-Palmitoyl-2-pyrenedecanoyl glycerophospholipids as membrane probes: Evidence for regular distribution in liquid-crystalline phosphatidylcholine bilayers, *Biochemistry 24*, 2773−2781.
21. Tang, D., and Chong, P. L.-G. (1992) E/M dips. Evidence for lipids regularly distributed into hexagonal super-lattices in pyrene-PC/DMPC binary mixtures at specific concentrations, *Biophys. J. 63*, 903−910.
22. Chong, P. L.-G. (1994) Evidence for regular distribution of sterols in liquid crystalline phosphatidylcholine bilayers, *Proc. Natl. Acad. Sci. U.S.A. 91*, 10069−10073.
23. Virtanen, J. A., Somerharju, P., and Kinnunen, P. K. J. (1988) Prediction of patterns for the regular distribution of substitutional impurities in liquid phase of lipid bilayer, *J. Mol. Electron. 4*, 233−236.
24. Liu, F., and Chong P. L.-G. (1999) Evidence for a regulatory role of cholesterol superlattices in the hydrolytic activity of secretory phospholipase A2 in lipid membranes, *Biochemistry 38*, 3867−3873.
25. Huang, J., and Feigenson, G. W. (1999) A microscopic interaction model of maximum solubility of cholesterol in lipid bilayers, *Biophys. J. 76*, 2142−2157.
26. Huang, J. (2002) Exploration of molecular interactions in cholesterol superlattices: Effect of multibody interactions, *Biophys. J. 83*, 1014−1025.
27. Dietrich, C., Bagatolli, L. A., Volovyk, Z. N., Thompson, N. L., Levi, M., Jacobson, K., and Gratton, E. (2001) Lipid rafts reconstituted in model membranes, *Biophys. J. 80*, 1417−1428.
28. Ahmed, S. N., Brown, D., and London, E. (1997) On the origin of sphingolipid/cholesterol-rich detergent-insoluble cell membranes: Physiological concentrations of cholesterol and sphingolipid induce formation of a detergent-insoluble, liquid-ordered lipid phase in model membranes, *Biochemistry 36*, 10944−10953.
29. Subczynskia, W. K., and Kusumi, A. (2003) Dynamics of raft molecules in the cell and artificial membranes: Approaches by pulse EPR spin labeling and single molecule optical microscopy, *Biochim. Biophys. Acta 1610*, 231−243.
30. Chong, P. L.-G, and Sugar, I. P. (2002) Fluorescence studies of lipid regular distribution in membranes, *Chem. Phys. Lipids. 116*, 153−175.
31. Wang, M. M., Olsher, M., Sugar, I. P., and Chong, P. L.-G. (2004) Cholesterol superlattice modulates the activity of cholesterol oxidase in lipid membranes, *Biochemistry 43*, 2159−2166.
32. Cannon, B., Hermansson, M., Györke, S., Somerharju, P., Virtanen, J. A., and Cheng, K. H. (2003) Regulation of calcium channel activity by lipid domain formation in planar lipid bilayers, *Biophys. J. 85*, 933−942.
33. Cornelius, F. (1995) Cholesterol modulation of molecular activity of reconstituted shark Na^+,K^+-ATPase, *Biochim. Biophys. Acta 1235*, 205−212.
34. Cornelius, F. (2001) Modulation of Na^+/K^+-ATPase and Na^+-ATPase activity by phospholipids and cholesterol. I. Steady-state kinetics, *Biochemistry 40*, 8842−8851.
35. Giraud, F., Claret, M., Bruckdorfer, K. R., and Chailley, B. (1981) The effects of membrane lipid order and cholesterol on the internal and external cationic sites of the Na^+-K^+ pump in erythrocytes, *Biochim. Biophys. Acta 647*, 249−258.
36. Yeagle, P. L. (1983) Cholesterol modulation of Na^+/K^+-ATPase ATP hydrolyzing activity in the human erythrocyte, *Biochim. Biophys. Acta 727*, 39−44.
37. Sotomayor, C. P., Aguilar, L. F., Cuevas, F. J., Helms, M. K., and Jameson, D. M. (2000) Modulation of pig kidney Na^+/K^+-ATPase activity by cholesterol: Role of hydration, *Biochemistry 39*, 10928−10935.
38. Jorgensen, P. L. (1974) Purification and characterization of Na^+/K^+-ATPase. III. Purification 02111 the outer medulla of mammalian kidney after selective removal of membrane components by sodium dodecylsulphate, *Biochim. Biophys. Acta 356*, 36−52.
39. Jorgensen, P. L. (1974) Purification of Na^+/K^+-ATPase: active site determinations and criteria of purity, *Ann. N.Y. Acad. Sci. 242*, 36−52.
40. Baginsky, E. S., Foà, P. P., and Zak, B. (1967) Microdetermination of inorganic phosphate, phospholipids, and total phosphate in biologic materials, *Clin. Chem. 13*, 326−332.
41. Lowry, O. H., Rosebrough, N. J., Lewis-Farr, A., and Randall, R. J. (1951) Protein measurement with the folin phenol reagent, *J. Biol. Chem. 193*, 265−275.
42. Cornelius, F., and Skou, J. C. (1984) Reconstitution of Na^+/K^+-ATPase into phospholipid vesicles with full recovery of its specific activity, *Biochim. Biophys. Acta 772*, 357−373.
43. Röschlau, P., Bernet, E., and Gruber, W. (1974) Enzymatic determination of total cholesterol in serum, *Z. Klin. Chem. Klin. Biochem. 12*, 403−407.
44. Zilversmith, D. B., and Davis, K. (1950) Test-combination phosphorus, phospholipids, *J. Lab. Clin. Med. 35*, 155−160.
45. Buhagiar, K. A., Hansen, P. S., Kong, B. Y., Clarke, R. J., Fernandez, C., and Rasmussen, H. H. (2004) Dietary cholesterol alters Na^+/K^+ selectivity at intracellular Na^+/K^+ pump sites in cardiac myocytes, *Am. J. Physiol. Cell Physiol. 286*, C398−C405.
46. Cornelius, F. (1988) Incorporation of C12E8-solubilized Na^+/K^+-ATPase into liposomes: Determination of sidedness and orientation, *Methods Enzymol. 156*, 156−167.
47. Ward, D., and Cavieres, J. (1996) Binding of 2′(3′)-O-(2,4,6-trinitrophenyl)ADP to soluble $\alpha\beta$ protomers of Na^+/K^+-ATPase modified with fluorescein isothiocyanate: Evidence for two distinct nucleotide sites, *J. Biol. Chem. 271*, 12317−12321.
48. Kapakos, J., and Steinberg, M. (1982) Fluorescent labeling of Na^+/K^+-ATPase by 5-iodoacetamidofluorescein, *Biochim. Biophys. Acta 693*, 493−496.
49. Spencer, R. D., and Weber, G. (1969) Measurement of subnanosecond fluorescence lifetimes with a cross-correlation phase fluorometer, *Ann. N.Y. Acad. Sci. 158*, 361−376.
50. Gratton, E., Jameson, D. M., and Hall, R. D. (1984) Multifrequency phase and modulation fluorometry, *Annu. Rev. Biophys. Bioeng. 13*, 105−124.
51. Jameson, D. M., and Hazlett, T. L. (1991) Time-resolved fluorescence measurements in biology and biochemistry, in *Biophysical and Biochemical Aspects of Fluorescence Spectroscopy*, pp 105−133, Plenum Press, New York.
52. Alcala, J. R., Gratton, E., and Prendergast, F. G. (1987) Resolvability of fluorescence lifetime distributions using phase fluorometry, *Biophys. J. 51*, 587−596.
53. Alcala, J. R., Gratton, E., and Prendergast, F. G. (1987) Fluorescence lifetime distributions in proteins, *Biophys. J. 51*, 597−604.
54. Alcala, J. R., Gratton, E., and Prendergast, F. G. (1987) Interpretation of fluorescence decays in proteins using continuous lifetime distributions, *Biophys. J. 51*, 925−936.
55. Klonis, N., and Sawyer, W. (2003) The thiourea group modulates the fluorescence emission decay of fluorescein-labeled molecules *Photochem. Photobiol. 77*, 502−509.
56. Lakowicz, J. R. (1999) *Principles of Fluorescence Spectroscopy*, 2nd ed., Kluwer Academic, New York.
57. Parasassi, T., De Stasio, G., d'Ubaldo, A., and Gratton, E. (1990) Phase fluctuation in phospholipid membranes revealed by Laurdan fluorescente, *Biophys. J. 57*, 1179−186.
58. Silvestro, L., and Axelsen, P. H. (1998) Infrared spectroscopy of supported lipid monolayer, bilayer, and multibilayer membranes, *Chem. Phys. Lipids 96*, 69−80.
59. Jorgensen, P. L. (1974) Purification and characterization of Na^+/K^+-ATPase. IV. Estimation of the purity and of the molecular weight and polypeptide content per enzyme unit in preparations from the outer medulla of rabbit kidney, *Biochim. Biophys. Acta 356*, 53−67.
60. Tyson, P. A., Steinberg, M., Wallick, E. T., and Kirley, T. L. (1989) Identification of the 5-iodoacetamidofluorescein reporter site on the Na^+/K^+-ATPase, *J. Biol. Chem. 264*, 726−734.
61. Muller, E., Giehl, A., Schwarzmann, G., Sandhoff, K., and Blume, A. (1996) Oriented 1,2-dimyristoyl-sn-glycero-3-phosphorylcholine/ganglioside membranes: a Fourier transform infrared attenuated total reflection spectroscopic study. Band assignments; orientational, hydrational, and phase behavior; and effects of Ca^{2+} binding, *Biophys. J. 71*, 1400−1421.
62. Lewis, R. N., McElhaney, R. N., Pohle, W., and Mantsch, H. H. (1994) Components of the carbonyl stretching band in the infrared spectra of hydrated 1,2-diacylglycerolipid bilayers: a reevaluation, *Biophys. J. 67*, 2367−2375.
63. Jackson, M., and Mantsch, H. H. (1995) The use and misuse of FTIR spectroscopy in the determination of protein structure, *Crit. Rev. Biochem. Mol. Biol. 30*, 95−120.

64. Parasassi, T., Conti, F., and Gratton, E. (1986) Time-resolved fluorescence emission spectra of Laurdan in phospholipid vesicles by multifrequency phase and modulation fluorometry, *Cell Mol. Biol. 32*, 103−108.
65. Parasassi, T., De Stasio, G., Ravagnan, G., Rusch, R. M., and Gratton, E. (1991) Quantitation of lipid phases in phospholipid vesicles by the generalized polarization of Laurdan fluorescence, *Biophys. J. 60*, 179−189.
66. Parasassi, T., Di Stefano, M., Loiero, M., Ravagnan, G., and Gratton, E. (1994) Cholesterol modifies water concentration and dynamics in phospholipid bilayers: a fluorescence study using Laurdan probe, *Biophys. J. 66*, 763−768.
67. Zannoni, C., Argioni A., and Cavatorta, P. (1983) Fluorescence depolarization in liquid crystals and membrane bilayers, *Chem. Phys. Lipids 32*, 179−250.
68. Rog, T., and Pasenkiewicz-Gierula, M. (2001) Cholesterol effects on the phosphatidylcholine bilayer nonpolar region: a molecular simulation study, *Biophys. J. 81*, 2190−2202.
69. Carilli, C. T., Farley, R. A., Perlman, D. M., and Cantley, L. C. (1982) The active site structure of Na^+- and K^+-stimulated ATPase. Location of a specific fluorescein isothiocyanate reactive site, *J. Biol. Chem. 257*, 5601−5606.
70. Karlish, S. J. (1980) Characterization of conformational changes in Na^+/K^+-ATPase labeled with fluorescein at the active site, *J. Bioenerg. Biomembr. 12*, 111−136.
71. Lupfert, C., Grell, E., Pintschovius, V., Apell, H. J., Cornelius, F., and Clarke, R. J. (2001) Rate limitation of the Na^+, K^+-ATPase pump cycle, *Biophys. J. 81*, 2069−2081.
72. Ovchinnikov, Y., Modyanov, N. N., Broude, N. E., Petrukhin, K. E., Grishin, A. V., Arzamazova, N. M., Aldanova, N. A., Monastyrskaya, G. S., and Sverdlov, E. D. (1986) Pig kidney Na^+/K^+-ATPase. Primary structure and spatial organization, *FEBS Lett. 201*, 237−245.
73. Lutsenko, S., Daoud, S., and Kaplan, J. H. (1997) Identification of two conformationally sensitive cysteine residues at the extracellular surface of the Na^+/K^+-ATPase alpha-subunit. *J. Biol. Chem. 272*, 5249−5255.
74. Kapakos, J. G., and Steinberg, M. (1986) Ligand binding to Na^+/K^+-ATPase labeled with 5-iodoacetamidofluorescein, *J. Biol. Chem. 261*, 2084−2089.
75. Klonis, N., Clayton, A. H., Voss, E. W., Jr., and Sawyer, W. H. (1998) Spectral properties of fluorescein in solvent-water mixtures: applications as a probe of hydrogen bonding environments in biological systems, *Photochem. Photobiol. 67*, 500−510.
76. Klonis, N., and Sawyer, W. H. (2000) Effect of solvent-water mixtures on the prototropic equilibria of fluorescein and on the spectral properties of the monoanion, *Photochem. Photobiol. 72*, 179−185.
77. Gangal, M., Cox, S., Lew, J., Clifford, T., Garrod, S. M., Aschbaher, M., Taylor, S. S., and Johnson, D. A. (1998) Backbone flexibility of five sites on the catalytic subunit of cAMP-dependent protein kinase in the open and closed conformations, *Biochemistry 37*, 13728−13735.
78. Kaiser, E. T., and Kézdy, F. J. (1983) Secondary structures of proteins and peptides in amphiphilic environments, *Proc. Natl. Acad. Sci. U.S.A. 80*, 1137−1143.
79. Macdonald, J. R., and Johnson W. C, (2001) Environmental features are important in determining protein secondary structure, *Protein Sci. 10*, 1172−1177.
80. Waterhous, D. V., and Johnson, W. C. (1994) Importance of environment in determining secondary structure in proteins, *Biochemistry 33*, 2121−2128.
81. Haris, P. I., and Chapman, D. (1996) in *Infrared Spectroscopy of Biomolecules* (Mantsch, H. H., and Chapman, D., Eds.) pp 239−278, Wiley-Liss, New York.
82. Jackson, M., Haris, P. I., and Chapman, D. (1991) Fourier transform infrared spectroscopic studies of Ca^{2+}-binding proteins, *Biochemistry 30*, 9681−9686.
83. Benkian, A., Malonga, H and Tajmir-Riahi, H. A. (2001) The effects of anions on the solution structure of Na^+/K^+-ATPase, *J. Biomol. Struct. Dyn. 19*, 95−102.
84. Neualt, J. F., Malonga, H, Diamantoglou, S., Carpentier, R., Stepp, R. L. and Tajmir-Riahi, H. A. (2002) Secondary structural analysis of the Na^+/K^+-ATPase and its Na^+ (E1) and K^+ (E2) complexes by FTIR spectroscopy, *J. Biomol. Struct. Dyn. 20*, 173−178.
85. Chetverin, A. B., Venyaminox, S. Y., Emelyanenko, V. I., and Burstein, E. A. (1980) Lack of gross protein structure changes in the working cycle of (Na^+, K^+)-dependent adenosinetriphosphatase. Evidence from infrared and intrinsic fluorescence spectroscopy data, *Eur. J. Biochem. 108*, 149−156.
86. Pratap, P. R., Dediu, O., and Nienhaus, G. U. (2003) FTIR study of ATP-induced changes in Na^+/K^+-ATPase from duck supraorbital glands, *Biophys. J. 85*, 3707−3717.
87. Menashe, M., Romero, G., Biltonen, R. L., and Lichtenbergs, D. (1986) Hydrolysis of dipalmitoylphosphatidylcholine small unilamellar vesicles by porcine pancreatic phospholipase A2, *J. Biol. Chem. 261*, 5328−5333.
88. Lichtenberg, D., Romero, G., Menashe, M., and Biltonen, R. L. (1986) Hydrolysis of dipalmitoylphosphatidylcholine large unilamellar vesicles by porcine pancreatic phospholipase A2, *J. Biol. Chem. 261*, 5334−5340.
89. Micol, V., Sanchez-Piñera, P., Villalain, J., De Godos, A., and Gomez-Fernandez, J. C. (1999) Correlation between protein kinase C α activity and membrane phase behavior, *Biophys. J. 76*, 916−927.

BI061351E